Experimental and Molecular Pathology 107 (2019) 179–183

Contents lists available at ScienceDirect

Experimental and Molecular Pathology

journal homepage: www.elsevier.com/locate/yexmp

Primary sclerosing epithelioid fibrosarcoma of the kidney: Report of two additional cases with a clinicopathological and molecular cytogenetic study

Xiaoxia Wang[a,*], Jian Wang[b]

[a] Department of Nephrology, Tongren Hospital Shanghai Jiao Tong University School of Medicine, Shanghai 200336, China
[b] Department of Pathology, Fudan University Shanghai Cancer Center, Shanghai 200032, China

ARTICLE INFO

Keywords:
Sclerosing epithelioid sarcoma
Kidney
Immunohistochemsitry
Florescence in site hybridization
EWSR1

ABSTRACT

We present two cases of sclerosing epithelioid fibrosarcoma (SEF) that arose primarily in the kidney. The tumor in both cases was located at the upper pole of the kidney. Clincially, they were suspected as renal cell carcinomas. However, histological examination revealed densely hyalinized epithelioid tumor suggestive of SEF. The diffuse immunohistochemical staining of MUC4 by neoplastic cells and the presence of *EWSR1* gene rearrangement by subsequent florescence in site hybridization (FISH) analysis confirmed the histological diagnosis. Molecular cytogenetic study is highly helpful in arriving at a final diagnosis, in particular to a rare tumor type that arises at an unusual site.

1. Introduction

Sclerosing eithelioid fibrosarcoma (SEF) is a rare variant of fibrosarcoma characterized by infiltrative cords, strands, nests or sheets of epithelioid cells embedded in a heavily hyalinized stroma (Meis-Kindblom et al., 1995). This tumor type is commonly encountered in young to middle aged adults without marked gender preference. It typically occurs in the deep soft tissue of extremities, followed by the trunk, head and neck region, and less frequentlly abdomen/pelvis, retroperitoneum and bone (Antonescu et al., 2001; Wojcik et al., 2014). Occurrence of a primary SEF in visceral organs is exceedingly rare which may cause diagnostic pitfalls both clinically and pathologically. We present here two cases of SEF that arose primarily in the kidney with a clinicopathological and molecular cytogenetic study.

2. Brief report

2.1. Case 1

The patient was a 37-year-old female who presented with occasional pain on her right upper abdomen for a period of one year. Her past medical history was unremarkable. B ultrasound revealed a low echo area measuring 50 × 45 mm in the right kidney. Computerized tomography scan of the upper abdomen showed a 57 × 47 × 44 mm mass at the middle to upper pole of the right kidney (Fig. 1A), which was suspected as renal cell carcinoma. The laboratory examinations were all in normal limits. Laparoscopic partical nephrectomy was performed. The patient recovered well after the surgery with adjunctive therapies. She is well with no signs of local recurence or distant metastasis at 11 month's follow up.

2.2. Case 2

The patient was a 45-year-old female who had polycystic kidney disease for a perioid of 4 years. Recently, she complaind of increasing left flank pain that radiated to her back. Physicl examination revealed a hard mass with tenderness in the left renal region. B ultrasound discovered a 106 × 69 mm hypoechic mass located at the upper pole of left kidney, in addition to anechoic cysts in bilateral kidneys. Computerized axial tomography scans showed a huge mass occupying the upper pole of the left kidney (Fig. 1B). A radical nephroectomy was carried out shortly after the admission of the patient. An adult nephroblastoma was considered initially by a local pathologist. Further histopathological examination with additional immunohistochemical and molecular cytogenetic studies revealed a SEF. The patient is currently well just one month after surgery. Additional chemotherapy was recommended due to the large size of the tumor.

2.3. Histology

Grossly, the excised tumor in case 1 measured 6 × 5 × 4.5 cm in size and was gray to pinkish with firm consistency on cut section. The

* Corresponding author.
E-mail address: ouyang1985@sjtu.edu.cn (X. Wang).

https://doi.org/10.1016/j.yexmp.2019.02.006
Received 30 December 2018; Received in revised form 24 January 2019; Accepted 25 February 2019
Available online 27 February 2019

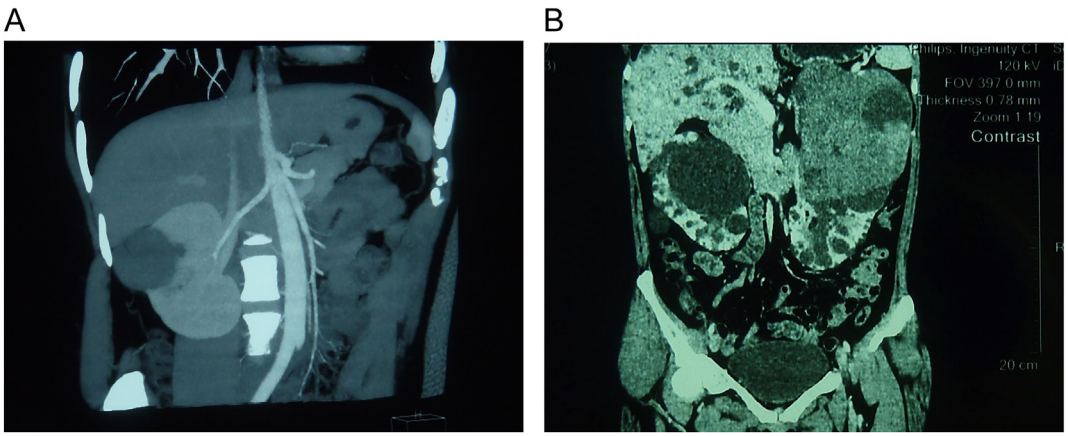

Fig. 1. Radiological features. A.CT scan in case 1 revealed a mass at the middle to upper pole of the right kidney. B. CT scan in case 2 showed a huge mass occupying the upper pole of the left kidney. Bilateral kidneys displayed polycystic disease.

specimen in case 2 was consisted of whole left kidney with adjacent adipose tissue measuring 20 × 11 × 11 cm in total. On cut section, a 16 × 11 × 11 cm grayish mass was found which occupied the entire upper pole of the kidney. The other areas of the kidney showed multiple cystic changes.

Microscopically, whereas the tumor in case 1 was relatively well circumscribed (Fig. 2A), the tumor in case 2 showed infiltration into the renal parechyma (Fig. 2B). Both tumors were composed of strands or cords of monotonous epithelioid cells with clear cytoplasm and angulated nuclei embedded in a heavily hyalinized stroma (Fig. 2C and D). In case 1, there were also alterating areas of high cellularity composed of compact nests, sheets of ovoid to epithelioid cells with clear cytoplasm, or compact fascicles of spindled cells reminiscent of a conventional fibrosarcoma (Fig. 2E). In case 2, there were associated myxoid areas composed of short spindle cells exhibiting a whorled architecture closely resembling a low grade fibromyxoid sarcoma (LGFMS) (Fig. 2F). However, hyalinizing large rossetes were not found. In both cases, there was no necrosis and the mitotic activity was scarce.

2.4. Immunohistochemistry

Immunohistochemical staining was performed on 4-μm thick unstained sections generated from paraffin-embedded blocks on Ventana Automated Immunostainer (BenchMarker Ultra, Ventana Medical System, Inc.) according to the manufacturer's manual. The panel of antibodies used in this study included pancytokeratin (AE1/AE3, 1:50; Dako), epithelial membrane antigen (EMA) (E29, 1:200; Dako), MUC4 (8G7,1:100; Abacam), bcl-2 (clone 124, 1:100; Dako), vimentin (V9, 1:100; Dako), Ki67 (MIB1, 1:150; Dako), CD99 (12E7, 1:100; Dako), CD34 (QBEnd 10, 1:100; Dako), ERG (EPR3864, prediluted;Ventana), CD10 (SP67, ready to use; Ventana), α-smooth muscle actin (α-SMA) (1A4, 1:200; Dako), desmin (clone D33, 1:250; Dako), S100 protein (polyclonal,1:2500; Dako), and PAX8 (MRQ-50, 1:50; Cell Marque). Appropriate positive and negative controls were run concurrently with all antibodies tested.

By immunohistochemistry, tumor cells in both cases were diffusely postive for MUC4, bcl-2 and vimentin (Fig. 3A and B), and negative for AE1/AE3, EMA, CD10, PAX8, desmin, α-SMA, CD34, S100 protein, and ERG. Weak staining of CD99 was noted in case 2. Ki67 index ranged from 5% to 20%.

2.5. Florescence in site hybridization

Interphase fluorescence in situ hybridization (FISH) study was carried out on 5-μm thick sections generated from formalin-fixed, paraffin embedded tissues for assessment of the *EWSR1* or *FUS* gene rearrangement. Briefly, the sections were incubated in a humidified chamber (HYBriteTM system; Vysis, Abbott, Des Plaines, IL) using dual color breakapart probes of *EWSR1* (22q12) and *FUS* (16p11) (HYBriteTM system; Vysis, Abbott, Des Plaines, IL) according to the manufacturer's protocol. The fluorescence signals were analyzed using an Olympus BX51 fluorescence microscope (Olympus, Tokyo, Japan). A total of 200 successive nuclei were assessed. The cut off level for score as positive was when at least 20% of the nuclei showed a break apart signal.

FISH assay showed rearrangment of *EWSR1* gene in both tumors (Fig. 3C). Besides, unbalanced rearrangement of *EWSR1* with loss of telomeric part was noted in case 2 (Fig. 3D). No evidence of *FUS* gene rearrangement was present in both cases (not shown).

3. Discussion

SEF is a distinctive variant of fibrosarcoma with a metastatic potential. Although the majority of SEF occur in somatic soft tissues, it can also affect unusual sites in particular the visceral organs. Up to present, reported invovlement by SEF included the ovary (Watanabe and Suzuki, 2004), cecum (Frattini et al., 2007), liver (Tomimaru et al., 2009), lung (Leisibach et al., 2012) and pancreas (Bai et al., 2013). Of note, the first case of primary renal SEF was documented in a small series which emphasized on the molecular study of SEF (Arbajian et al., 2014). Since then, seven well-described cases have been reported in the English literature (Argani et al., 2015; Ohlmann et al., 2015; Ertoy Baydar et al., 2015; Torabi et al., 2017) (Table 1). Embracing the current two cases, there are 7 females and 3 males in total with age ranging from 16 to 61 years (mean, 37; median, 39 years) (Table 1). The left kidney was affected in 6 cases, whereas the right kidney was involved in 3 cases. The laterality in one case was not mentioned. The tumor measured 4.2 to 25 cm in maximum diameter, with a mean and median size of 11.7 cm and 7.5 cm respectively.

Clinically, patients usually presented with flank, abdominal or back pain. Radiological examinations (ultrasonography, CT and magnetic resonance tomogram) usually revealed a solid mass with soft tissue density located most commonly at the upper pole of the kidney, with some cases showing bulging through the renal capsule into perirenal fat, or encasement of the adrenal gland by the tumor (Ohlmann et al., 2015;). At initial presentation, 3 cases had synchronous metastatic disease (Argani et al., 2015; Ertoy Baydar et al., 2015). On histologic examination, reported cases of renal SEF showed similar morphology. They were all characterizaed by cords of polygonal or epithelioid cells with angulated nuclei and clear cytoplasm in a background of hyaline sclerosis, frequently entrapping the renal tubules or encicled the renal glomerulus (Argani et al., 2015; Ertoy Baydar et al., 2015). However,

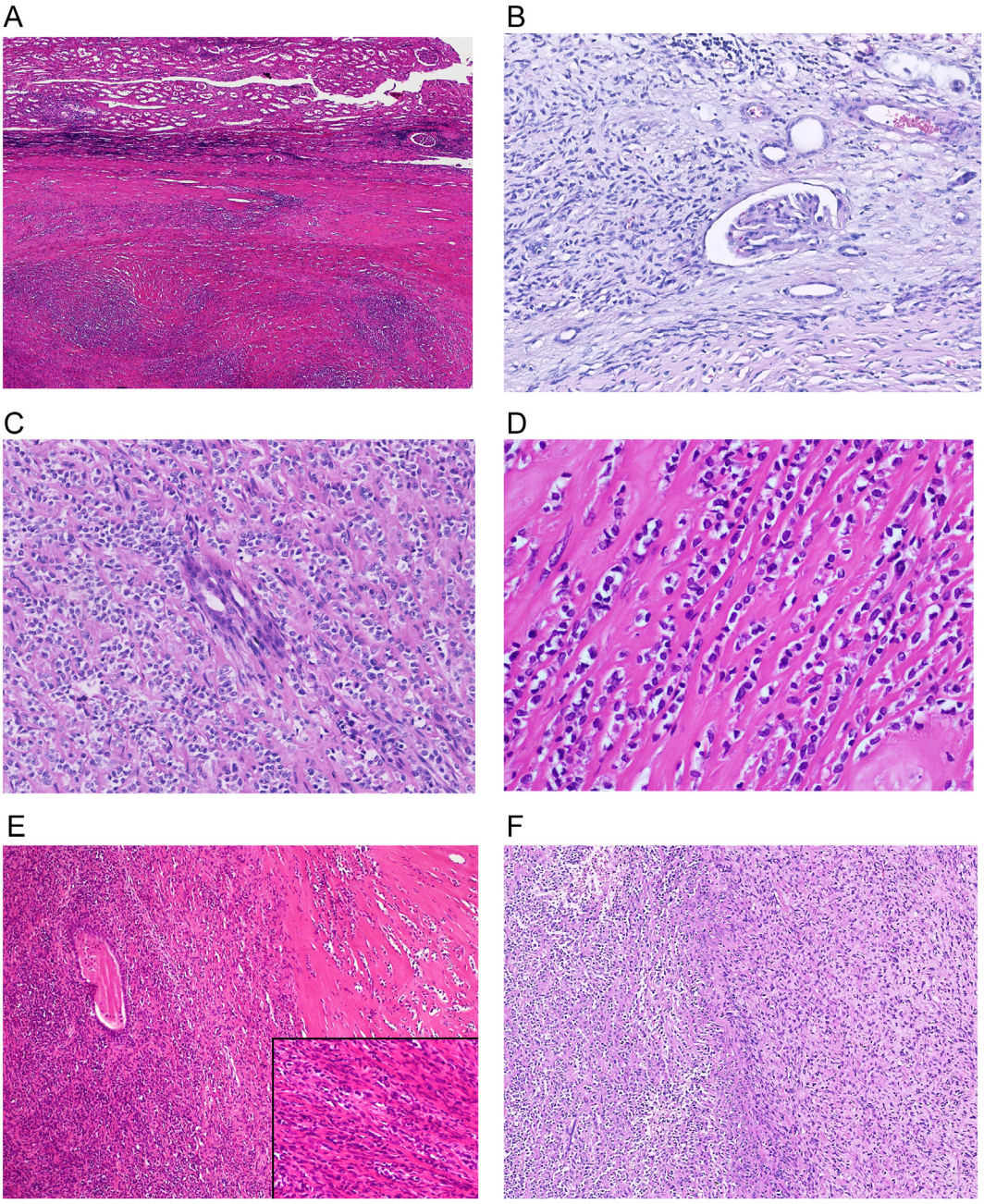

Fig. 2. Microscopic features. A. The tumor in case 1 was relatively well circumscribed. (H&E, original magnification, 40×) B. Tumor cells in case 2 infiltrated the renal parechyma. (H&E, original magnification, 200×) C. Monotonous epithelioid cells arranged in cords in case 2. (H&E, original magnification, 200×) D. Polygonal to epithelioid cells with clear cytoplams and angulated nuclei embedded in a heavily hyalinized stroma. (H&E, original magnification, 400×) E. Alterating areas of high cellularity resembling conventional fibrosarcoma (inset). (H&E, original magnification, 100×) F. Alterating myxoid areas mimicking a low grade fibromyxoid sarcoma. (H&E, original magnification, 100×).

there was always variable cellularity within the tumors, with abrupt transitions from areas of high cellularity to highly sclerotic areas of low cellularity. Hypercellular areas were composed of relatively compact nests, sheets or lobules of oval to epithelioid cells. Vague nodules of collagen mimicking those seen in hyalinizing spindle cell tumor with giant rosettes were occasionally noted (Argani et al., 2015; Ertoy Baydar et al., 2015). A focal myxoid nodule in one reported case (Argani et al., 2015) and alternative myxoid areas in one of our two cases (case 2) reminiscent of LGFMS were present but not sufficient for diagnosis of a hybrid SEF/LGFMS. Most recently, Mok et al. reported a particular case of hybrid renal LGFMS-SEF, of which the primary renal tumor showed features of a LGFMS but the cervical metastasis displayed the morphology of a SEF (Mok et al., 2018). Besides the sclerotic stroma, foci of calcification and metaplastic bone were present in 1 case (Torabi et al., 2017) and 2 cases (Argani et al., 2015) of SEF respectively. Mitotic figures in SEF were usually rare to absent.

Immuhistochemically, tumor cells in all reported cases of renal SEF showed diffuse staining for MUC4, a highly senstive and specific marker for SEF. Besides MUC4, expression of vimentin and bcl-2 was also frequently reported in SEF, but these two markers were generally considered as not tumor type-specific. Variable staining of EMA and CD99 were also noted in some cases of SEF, but again not diagnostic. SEF was consistently negative for pankeratin, PAX8, desmin, α-SMA, CD34, S100 protein, ERG, HMB45, GATA3, and CD117. The negativity of abovementioned markers may help the separation of SEF from its mimics.

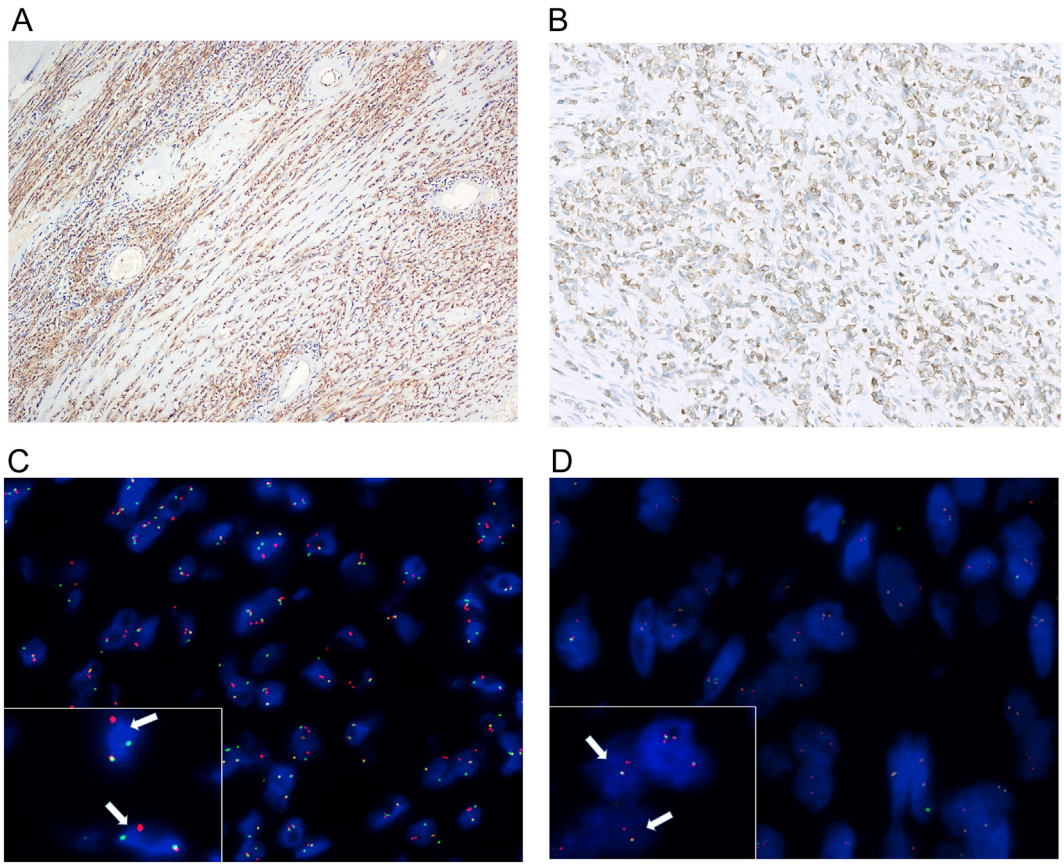

Fig. 3. Immunohistochemical features and FISH results. Tumor cells showed diffuse cytoplasmic positivity for MUC4 (A) and bcl-2 (B), with split of EWSR1 gene (C, white arrows) and loss of telomeric part (D, white arrows).

At molecular level, the majority of SEF harboured a reciprocal chromosomal translocation t(11;22)(p11;q12) resulting in generation of *EWSR1-CREB3L1 f*usion gene (Arbajian et al., 2014). Only a minority of SEF showed *EWSR1-CREB3L2* fusion gene, or less commonly *FUS-CREB3L2* fusion gene (Prieto-Granada et al., 2015). Thus, detection of *EWSR1* gene rearrangment by molecular assay is considered highly helpful in in the diagnosis and differential diagnosis of SEF in particular to those that arise at visceral organs. Currently, FISH using *EWSR1* break-apart probe is widely applied in routine practice. It has been noted that besides the split of *EWSR1* gene, there is also unbalanced rearrangement of *EWSR1* gene with loss of telomeric part, as illustrated in case 2 as well as in previously reported cases (Argani et al., 2015; Torabi et al., 2017). The fusion partner of *EWSR1* can be identified by further using custom dual fusion probe or by reverse transcription-polymerase chain reaction (RT-PCR) with designed primers. Among the reported cases of renal SEF, five cases demonstrated the presence of *EWSR1-CREB3L1* fusion gene (Argani et al., 2015; Ertoy Baydar et al., 2015; Torabi et al., 2017), but none of them was subsequently analysized for gene sequencing. Up to present, involvement of exons of *EWSR1* in SEF of somatic soft tissues included exon 7, 8 and 11

Table 1
Summary of clinicopathological features of primary renal SEF.

Authors	Age(yrs)/ Sex	Laterality	Size (cm)	Clinical features	FISH assay (Split apart/fusion)	MUC4 (IHC)	Follow-up (relapse/metastases)	Outcome (mo)
Arbajian et al.	41/F	NA	9	NA	Deletions of *EWSR1*	+	Lung and bone	DOD, 22
Argani et al.	17/M	Left	25	Left flank, back and abdominal pain	*EWSR1-CREB3L1*	+	Rib, vertbrae, epidural spinal cord and liver	DOC, 1
	61/F	Left	5	Rib pain	*EWSR1-CREB3L1*	+	Ribs, bone, lung and lymph nodes	AWD, 6
Ohlmann et al.	24/F	Right	22	NA	No result	+	Both lungs and vertebrae	DOD, 82
	43/M	Right	4.2	Incidental	Split apart of *EWSR1*	+	None	ANED, 8
Ertoy Baydar et al.	16/F	Left	7.5	Abdominal pain	*EWSR1-CREB3L1*	+	Lungs,vertebrae, sarcum and left femoral head	AWD, 30
	57/F	Left	7.5	Incidental	*EWSR1-CREB3L1*	+	None	ANED, 10
Torabi et al.	30/M	Left	15	Left flank pain	*EWSR1-CREB3L1*	+	Relaspsed/lymph node	
Wang et al. (current case)	37/F	Right	6	Occasion upper abdominal pain	Split apart of *EWSR1,*	+	None	ANED, 11
Wang et al. (current case)	45/F	Left	16	Left flank pain	Split apart of *EWSR1* with loss of telomeric part		None	ANED, 2

ANED, alive without evidence of disease; AWD, alive with disease; DOC, died of complications; DOD, died of disease; IHC, immunohistochemistry; NA, not available; ND, not done; SEF, sclerosing epithelioid fibrosarcoma.

(Arbajian et al., 2014; Stockman et al., 2014; Torabi et al., 2017), fused to exon 6 of *CREB3L1* gene.

In general, SEF has an aggressive clinical course with high rates of local recurrence (50%), distant metastasis (40–80%) and mortality (25–57%) (Meis-Kindblom et al., 1995; Antonescu et al., 2001). Of 10 renal SEF, metastases were present in 4 cases at the time of diangosis. Main sites of metastases were lung, liver, epidural spinal cord, bone (rib, vertebra, left femoral head, sarcum), and lymph nodes. Two patients died of disease at 22 months and 1 month. One patient died of disease complication at 82 months. Two patients were alive with disease at 6 months and 8 months respectively. The other 4 paitents were alive without evidence of local recurrence of distant metastasis, 2 of which had limited follow up (8 and 2 months). At present, surgery remains the mainstay of treatment in SEF. Aggressive multimodality treatment has been considered in patients with disseminated disease despite resistance to conventional chemotherapy and irradiation. In a recent study, SNP array analysis detected recurrent structural aberrations, particulary DMD microdeletions (Arbajian et al., 2017). In addition, CD24 was strongly upregulated in those harboring EWSR1-CREB3L1, suggesting a direct target of the fusion proteins. Whether CD24 and DMD constitute promising therapeutic targets in SEF warrants further studies.

The differential diagnosis of a renal SEF embraces a a variety of tumors with epithelioid morpholgy and sclerosing matrix, including sclerosing perivascular epithelioid cell tumor (PEComa) (Zhao et al., 2014), sclersoing variant of clear cell renal cell carcinoma of kidney (CCSK), Wilms tumor, metanephric stromal tumor (Argani and Beckwith, 2000), and rarely renal solitary fibrous tumor (Kuroda et al., 2014). The distinction has been well discussed in previous studies. With combination of morphology, MUC4 immunostaining and FISH anaylsis for the presence of *EWSR1* rearrangement, a precise diagnosis can be reached in SEF with atypical clinical presentations.

Conflicts of interest

The authors state that there are no conflicts of interest with respect to the research, authorship, and/or publication of this article.

Sources of funding

This study was supported in funding by National Natural Science Foudation of China (81270814, 81770718) and Shanghai Key Developing Disciplines (2015ZB0201).

References

Antonescu, C.R., Rosenblum, M.K., Pereira, P., et al., 2001. Sclerosing epithelioid fibrosarcoma. A study of 16 cases and confirmation of a clinicopathologically distinct tumor. Am. J. Surg. Pathol. 25 (6), 699–709.
Arbajian, E., Puls, F., Magnusson, L., et al., 2014. Recurrent EWSR1-CREB3L1 gene fusions in sclerosing epithelioid fibrosarcoma. Am. J. Surg. Pathol. 38 (6), 801–808.
Arbajian, E., Puls, F., Antonescu, C.R., et al., 2017. In-depth genetic analysis of sclerosing epithelioid fibrosarcoma reveals recurrent genomi alterations and potential treatment targets. Clin. Cancer Res. 23 (23), 7426–7434.
Argani, P., Beckwith, J.B., 2000. Metanephric stromal tumor: report of 31 cases of a distinctive pediatric renal neoplasm. Am. J. Surg. Pathol. 24 (7), 917–926.
Argani, P., Lewin, J.R., Edmonds, P., et al., 2015. Primary renal sclerosing epithelioid fibrosarcoma: report of 2 cases with EWSR1-CREB3L1 gene fusion. Am. J. Surg. Pathol. 39 (3), 365–373.
Bai, S., Jhala, N., Adsay, N.V., Wei, S., 2013. Sclerosing epithelioid fibrosarcoma of the pancreas. Ann. Diagn. Pathol. 17 (2), 214–216.
Ertoy Baydar, D., Kosemehmetoglu, K., Aydin, O., et al., 2015. Primary sclerosing epithelioid fibrosarcoma of kidney with variant histomorphologic features: report of 2 cases and review of the literature. Diagn. Pathol. 10, 186.
Frattini, J.C., Sosa, J.A., Carmack, S., Robert, M.E., 2007. Sclerosing epithelioid fibrosarcoma of the cecum: a radiation-associated tumor in a previously unreported site. Arch. Pathol. Lab Med. 131 (12), 1825–1828.
Kuroda, N., Ohe, C., Sakaida, N., et al., 2014. Solitary fibrous tumor of the kidney with focus on clinical and pathobiological aspects. Int. J. Clin. Exp. Pathol. 7 (6), 2737–2742.
Leisibach, P., Weder, W., Soltermann, A., Jungraithmayr, W., 2012. Primary sclerosing epithelioid fibrosarcoma of the lung in a patient with Lynch syndrome. Lung 190 (6), 691–695.
Meis-Kindblom, J.M., Kindblom, L.G., Enzinger, F.M., 1995. Sclerosing epithelioid fibrosarcoma. A variant of fibrosarcoma simulating carcinoma. Am. J. Surg. Pathol. 19 (9), 979–993.
Mok, Y., Pang, Y.H., Sanjeev, J.S., et al., 2018. Primary renal hybrid low-grade fibromyxoid sarcoma-sclerosing epithelioid fibrosarcoma: an unusual pediatric case with ewsr1-creb3l1 fusion. Pediatr. Dev. Pathol. 21 (6), 574–579.
Ohlmann, C.H., Brecht, I.B., Junker, K., et al., 2015. Sclerosing epithelioid fibrosarcoma of the kidney: clinicopathologic and molecular study of a rare neoplasm at a novel location. Ann. Diagn. Pathol. 19 (4), 221–225.
Prieto-Granada, C., Zhang, L., Chen, H.W., et al., 2015. A genetic dichotomy between pure sclerosing epithelioid fibrosarcoma (SEF) and hybrid SEF/low-grade fibromyxoid sarcoma: a pathologic and molecular study of 18 cases. Genes Chromosomes Cancer 54 (1), 28–38.
Stockman, D.L., Ali, S.M., He, J., et al., 2014. Sclerosing epithelioid fibrosarcoma presenting as intraabdominal sarcomatosis with a novel EWSR1-CREB3L1 gene fusion. Hum. Pathol. 45 (10), 2173–2178.
Tomimaru, Y., Nagano, H., Marubashi, S., et al., 2009. Sclerosing epithelioid fibrosarcoma of the liver infiltrating the inferior vena cava. World J. Gastroenterol. 15 (33), 4204–4208.
Torabi, A., Corral, J., Gatalica, Z., et al., 2017. Primary renal sclerosing epithelioid fibrosarcoma: a case report and review of the literature. Pathology 49 (4), 447–450.
Watanabe, K., Suzuki, T., 2004. Epithelioid fibrosarcoma of the ovary. Virchows Arch. 445 (4), 410–413.
Wojcik, J.B., Bellizzi, A.M., Dal Cin, P., et al., 2014. Primary sclerosing epithelioid fibrosarcoma of bone: analysis of a series. Am. J. Surg. Pathol. 38 (11), 1538–1544.
Zhao, Y., Bui, M.M., Spiess, P.E., Dhillon, J., 2014. Sclerosing PEComa of the kidney: clinicopathologic analysis of 2 cases and review of the literature. Clin. Genitourin Cancer 12 (5), e229–e232.